九州工業大学学術機関リポジトリ

Kyutacar

Kyushu Institute of Technology Academic Repository

High visible-light active Ir-doped-TiO2 brookite photocatalyst synthesized by hydrothermal microwave-assisted process

High visible-light active Ir-doped-TiO$_2$ brookite photocatalyst synthesized by hydrothermal microwave-assisted process

Víctor M. Menéndez-Flores[a,b,*], Teruhisa Ohno[b,c,d]

[a] *Graduate School of Engineering, Nagoya University, Chikusa-ku, Nagoya 464-8603, Japan*
[b] *Department of Applied Chemistry, Faculty of Engineering, Kyushu Institute of Technology, 1-1 Sensuicho, Tobata, Kitakyushu 804-8550, Japan*
[c] *JST, PRESTO, 4-1-8 Honcho Kawaguchi, Saitama 332-0012, Japan*
[d] *JST, ACT-C, 4-1-8 Honcho Kawaguchi, Saitama 332-0012, Japan*

a b s t r a c t

Iridium-doped TiO$_2$ having a brookite phase was synthesized as a visible light-active photocatalyst. It was prepared by using a hydrothermal assisted-microwave process as an improved competitive production method over the traditional hydrothermal process. The prepared materials were tested for decomposing

acetaldehyde or toluene in gas phase under visible light irradiation (入 455 nm), and they showed a strong

photocatalytic activity response. The activity of the prepared brookite TiO$_2$ material was optimized by adjusting the concentration of iridium ions as a dopant. The photocatalytic efficiencies of all of the pre-pared Ir-doped-TiO$_2$ photocatalysts were higher than the values obtained from commercially available visible-light responsive photocatalysts under the same experimental conditions

1. Introduction

Many attempts have been made to obtain safe and efficient semiconductor materials with high conducting properties. An appropriate material is the polymorph titanium dioxide due to its reduction–oxidation qualities, safety and stability [1]. The three TiO$_2$ crystal phases, anatase, rutile and brookite, have been rig- orously studied. Rutile TiO$_2$ and anatase TiO$_2$ have been mainly studied. Although the structure of brookite, TiO$_2$ was determined by Pauling and Sturdivant in 1928, preparation of pure brookite TiO$_2$ powder required longer investigations [2–9]. The difficulty in preparing brookite TiO$_2$ having both high purity and a large surface area is probably one of the reasons for the limited appli- cation of brookite TiO$_2$ as a photocatalyst. Nevertheless, the TiO$_2$ brookite phase has recently received attention as a photocatalyst material because of its band gap, morphology and optical char- acteristics. It has to be particularly pointed out the importance of brookite TiO$_2$ phase, since it contains the highest oxidation potential in comparison with the other two different TiO$_2$ crystal phases brookite (−0.46 V), anatase (−0.45 V) and rutile (−0.37 V[10]. Photocatalysis and nanotechnology have been closely related to develop different doping semiconductor strategies for achieving solar range applications in order to use visible light irradiation. In this present study, we prepared visible light-responsive brookite TiO$_2$ by iridium doping. Iridium oxides have various applications, including applications in cardiovascular medicine and neural stim- ulation, because of their charge injection properties and non-toxic effects[11]. The photocatalytic efficiency of the newly prepared photocatalyst was evaluated under visible light irradiation > (入 455 0.1 nm). Iridium doped TiO$_2$ having a brookite phase was prepared by a microwave-assisted hydrothermal process [12–15].)

±

2. Experimental

2.1. Chemicals

All chemical reagents used in the present study were commer- cial products without further treatments. A titanium precursor (titanium-ethoxide) was purchased from Sigma-Aldrich. Other chemicals were purchased from Wako Co. Ltd. (all of reagent grade). Glycolic acid was employed to control the crystallinity and morphology of brookite TiO_2 particles. $IrCl_3$ was used as dopant precursor. Commercial photocatalysts N- or S-doped TiO_2 anatase phase materials were used as reference for the comparison of acetaldehyde decomposition. The surface areas of N-doped TiO_2(Sumitomo Chemical Co. Ltd.) and S-doped TiO_2 (TOHO Titanium Co. Ltd.) were 97.4 $m^2 g^{-1}$ and 82.5 $m^2 g^{-1}$, respectively.

2.2. Preparation of Ir-doped TiO_2 having a brookite phase

Brookite TiO_2 was prepared in a microwave apparatus (Wave Magic Eyela MWO-1000S/500W). One cm^3 of titanium (IV) ethox- ide and ethanol was added to Milli-Q water with vigorous stirring, and the mixture was stirred for 30 min at room temperature. The resulting precipitate was centrifugally separated from the solution and dried under reduced pressure. The obtained titanium hydrox- ide particles were dispersed in Milli-Q water and then irradiated by ultrasonication. Then 30% hydrogen peroxide was added, and yellow peroxo titanic acid (PTA) solution was obtained. Ammo- nium (NH_3) solution as a pH-adjusting agent and glycolic acid as a shape-control reagent were then added to the solution. After stir- ring the solution at ca. 60 °C for 24 h, the solution in a Teflon bottle sealed with a stainless jacket was introduced into the microwave apparatus with diverse $IrCl_3$ concentrations.

Diverse conditions like reaction time, stirring speed, pH, power and glycolic acid as well as content of iridium were tested to opti- mize the photonic efficiency of Ir-TiO_2 brookite.

The reaction in the microwave apparatus was carried out at 200 °C without stirring, adjusted to pH10 using a power energy of
500 watts for 7 min.

2.3. Characterization

The specific surface area was determined with a surface area analyzer (Quantachrome, Autosorb-1) by using the Brunauer- Emmett-Teller (BET) method. The crystal structures of the samples

were confirmed by using an X-ray diffractometer (Rigaku, Mini- Flex II) with Cu K a radiation (λ

1.5405 Å). The morphology of the samples was observed by transmission electron microscopy (TEM; Hitachi, H-9000NAR).

2.4. Photocatalytic decomposition of acetaldehyde or toluene in gas phase

Photocatalytic activities of the photocatalysts were evaluated by the decomposition of acetaldehyde or toluene in gas phase. Ir- doped TiO_2 particles (100 mg) were spread on a glass dish, and the glass dish was placed into a Tedlar bag (AS ONE Co. Ltd.) with a vol- ume of 125 cm^3. Then 500 ppm of gaseous acetaldehyde or 100 ppm toluene was injected into the Tedlar bag in a mixture of synthetic air (20% O_2 and 80% N_2). Photo-irradiation was carried out at room temperature after the acetaldehyde or toluene adsorption equilib- rium had been reached. An LED lamp (λ 455 $\pm$ 0.1 nm) was used as a light source. The light intensity was adjusted to 1 mW cm^{-2}. Con- centrations of acetaldehyde, toluene and carbon dioxide (CO_2) were estimated by gas chromatography auto-sampler Agilent Technolo- gies 3000A Micro GC (Thermal conductivity detector). Before the evaluation, all of the TiO_2 samples were pretreated by black light irradiation in order to remove contaminants on the TiO_2 surface.

3. Results

3.5. Photocatalyst characterization

The specific surface areas of Ir-doped TiO_2 brookite mate- rials 0.25; 0.5; 0.75 and 1.5 wt% corresponding, respectively to (172.13 m^2 g^{-1}); (208.41 m^2 g^{-1}) (219.67 m^2 g^{-1}) and (231.15 m^2 g^{-1}) or the undoped brookite (128.18 m^2 g^{-1}) were measured by the BET method and compared to the commercially available visible light-responsive TiO_2 photocatalysts (S-doped TiO_2 and N-doped TiO_2). The surface area of bare brookite TiO_2 was higher than those of reference photocatalysts (S-doped TiO_2 and N-doped TiO_2). Among the photocatalysts, the Ir-doped brookite TiO_2 showed the highest specific surface. The surface area was increased by doping TiO_2 with Ir due to the interstitial spaces formed in the TiO_2 lattice by insertion of Ir atoms.

Fig. 1 shows the normalized diffuse reflectance spectra of bare brookite TiO_2, N-doped TiO_2, S-doped TiO_2 and Ir-doped TiO_2 brookite synthesized photocatalysts (Ir-TiO_2). A clear red shift in the absorption edge of the Ir-doped brookite TiO_2 was observed compared to the bare brookite TiO_2.

The band gap energy of the prepared bare brookite TiO_2 material (3.14 eV) (Fig. 2) was determined by the Kubelka-Munk function $[F(R)hv]^{1/2}$. Moreover, the impurity energy level of the Ir-doped brookite TiO_2 was found to be in the visible region (1.88 eV) (Fig. 2 inserted graph). High absorption of visible light by the Ir-doped brookite TiO_2 photocatalyst can be predicted.

The flatband potentials of semiconductor electrodes at the semiconductor/electrolyte junction can be obtained from Mott- Schottky plots (measured in the dark) [Eq. (1)] [16,17].

$$\frac{1}{C^2} = \frac{2}{\varepsilon_{TiO_2} \cdot \varepsilon_0 \cdot e_0 \cdot N_D} \cdot \left(E - E_{FB} - \frac{kT}{e_0} \right), \qquad (1)$$

where ε_0 is the permittivity of free space, ε_{TiO2} is the permittivity of the semiconductor electrode, e_0 is the elementary charge, N_D is donor density, E is applied potential, E_{FB} is flatband potential, k is the Boltzmann constant, T is temperature of the operation, and C is space charge capacitance.

The flatband potentials have been measured by impedance spec- troscopy using Mott-Schottky plots. TiO_2 nanomaterial paste for the fabrication of electrodes for impedance measurements was obtained by mixing 1 mL of water and 100 mg of TiO_2 nanomaterial powder homogeneously by sonication. An appropriate amount of the TiO_2 suspension was spread on a conductive fluorine-tin oxide glass with a glass rod, followed by drying in air at 100 °C for 2 h. The electrical contact was formed on the uncoated area of the substrate using silver paint and copper wire. The electrochemical setup for impedance measurements consisted of three electrodes: the work- ing electrode (TiO_2 film), a platinum wire used as counter electrode, and Ag/AgCl, NaCl (3.0 M) electrode as reference (+0.21 vs NHE). The experiments were performed in aqueous 0.1 M KCl solutions at pH 7.

The Mott-Schottky plot for TiO_2 brookite nanoparticles is shown in Fig. 3. The results indicate that the E_{FB} is 0.766 V (vs Ag/AgCl). Kandiel et al. [9] obtained similar results of quasi-Fermi brookite levels of −0.77 V (vs NHE). In this study after doping brookite with iridium no significant E_{FB} change was found presumably due to the low iridium doping weight percent.

The crystal structure of Ir-doped TiO_2 was assigned to the brookite phase by XRD analyses (Fig. 4). The XRD pattern of Ir-doped-TiO_2 having a brookite phase shows a high level of crystallinity after the microwave-assisted hydrothermal process at 200 °C for 7 min. With higher concentrations than 0.5% of iridium as dopant, the intensity of the brookite peaks can be modified (Fig. 4(d)).

The morphology of synthesized TiO_2 nanoparticles was studied by TEM analyses. There is no clear difference between the pre- pared doped or undoped brookite TiO_2 materials. The Ir-doped brookite TiO_2 showed a rod-like shape with an average size of 10 nm (Fig. 5). The size of Ir-doped brookite TiO_2 nanoparticles is due to the microwave process with a short reaction time. An advantage of this particles size is their large surface area.

The XPS peaks of the prepared Ir-doped brookite TiO_2 were performed in order to elucidate the Ir cation doping condition in the TiO_2 lattice. XPS peaks assigned to Ir cations were observed. After Ar etching, the peaks of Ir cations remained (Fig. 6). These results strongly indicate that Ir cations should be located in the lattice of TiO_2. The best fit of the peaks yielded two oxidation states, which were attributed, respectively to Ir^{III} at 59.6 and to Ir^{IV} at 61.5. These results are shifted 1.1 eV from the corresponding 61.7 eV and 62.6 eV due to the doping procedure.
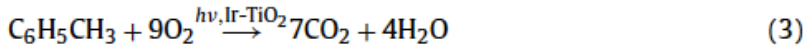
3.2. Photocatalytic decomposition of acetaldehyde under visible light using Ir-doped brookite TiO_2

The contents of Ir cations in TiO_2 were optimized by using different Ir concentrations, from 0.25% up to 1.5% in relation to TiO_2 weight. When 0.5 wt% of Ir cations was doped into the brookite TiO_2, the highest photocatalytic activity of Ir-doped brookite TiO_2 was observed for decomposition of acetaldehyde in gas phase under visible light (λ 455 nm) (Fig. 7) [Eq. (2)]. In all cases the activity of the self-prepared Ir-doped brookite TiO_2 was superior to that of the commercial S- or N-doped TiO_2 photocatalysts under the same reaction conditions. A possible reason for the fast initial decomposition reaction by the application of brookite TiO_2 phase compared to anatase or rutile might be due to its higher oxidation potential able to produce $O_2^{\bullet-}$ radicals and formally trapped Ti-$^{\bullet}$OH (Fig. 8). On the other hand decomposition processes with commercial photo- catalysts takes place mainly only on the surface of the materials.

$$CH_3CHO + \tfrac{5}{2}O_2 \xrightarrow{h\nu,\,Ir\text{-}TiO_2} 2CO_2 + 2H_2O \qquad (2)$$
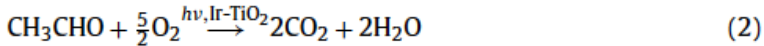
3.3. Photocatalytic decomposition of toluene under visible light using iridium-doped brookite TiO_2

Photodegradation of toluene in gas phase over TiO_2 was also evaluated under visible light irradiation. Toluene was selected as a toxic and recalcitrant compound to show the important potential application of the developed photocatalytic material. Brookite TiO_2 doped with 0.5 wt% Ir cations was found to be the most active photocatalyst among the photocatalysts with different iridium quantities (0.25 wt%, 0.5 wt%, 0.75 wt% and 1.5 wt%), (Fig. 9) [Eq. (3)]. Photocatalysts with higher iridium concentrations showed lower photocatalytic decomposition rates.

$$C_6H_5CH_3 + 9O_2 \xrightarrow{h\nu,\,Ir\text{-}TiO_2} 7CO_2 + 4H_2O \qquad (3)$$

3.4. Photonic efficiencies by decomposition of acetaldehyde or toluene

Photonic efficiency is defined as the ratio of the initial degrada- tion rate (k) divided by the incident photon flux [Eqs. (4) and (5)] [18,19]. The incident photon flow was determined from UV-A light meter measurements (1 mW cm^{-2}) by using an LED lamp with λ 455 nm. Photonic efficiencies were calculated for the decomposi- tion of acetaldehyde and toluene for comparison of the different photocatalysts.

$$J_0 = \frac{I \cdot \lambda}{N_A \cdot h \cdot c}, \qquad (4)$$

$$PE = \frac{k \cdot c_0 \cdot V}{J_0 \cdot A} \cdot 100. \qquad (5)$$

J_0 = photon flux intensity [mol s^{-1} cm^{-2}]; I = incident light inten- sity [J s^{-1} cm^{-2}]; λ = wavelength [nm]; N_A = Avogadro's number [$6.022 \cdot 10^{23}$ mol^{-1}]; h = Planck constant [$6.63 \cdot 10^{-34}$ J s]; c = light velocity [m s^{-1}]; k = rate constant [s^{-1}]; A = area [cm^2]; and c_0 = initial$_{Acetaldehyde/Toluene}$ concentration [mol L^{-1}]; V = volume [L]

Table 1 shows the photonic efficiencies of the photocatalysts under visible light LED lamp (λ 455 nm) irradiation used for degra- dation of acetaldehyde and toluene, respectively. The pollutant concentration in the case of acetaldehyde was 500 ppm and that in the case of toluene was 100 ppm by using 0.1 g of the photo- catalyst in each case. As can be seen in Table 1, a comparison of commercial N-doped TiO_2 and S-doped TiO_2 photocatalysts with the self-prepared photocatalysts

showed that a considerably higher photonic efficiency (0.69%) could be obtained by using the 0.5% Ir-doped TiO_2 photocatalyst.

4. Discussion

4.1. Origin of visible light activity

The surface states of semiconductor materials can play an important role in the photocatalytic activity. Surface states are caused by incomplete covalent bonds at the surface of the semicon- ductor and result in electron energy levels within the energy band gap. When electrons and holes are trapped in the surface states, the spatial overlap of charge carriers is reduced, retarding their recombination due to the localized nature of local states. There- fore, abundant surface states can greatly promote the separation of photoexcited electron–hole pairs. Morphology, size, defects and dopants are important factors affecting the surface atomic structure nd, therefore, the surface states of photocatalysts. Manipulation of surface states depends on control of the surface atomic structure [20]. Although precise control of the surface atomic structure is very difficult, it is possible to develop some strategies to increase/decrease the number of surface states. Many studies have been devoted to improvement of photocatalytic efficiency of TiO_2 by using various methods such as deposition of noble metals [19]. The deposition of a noble metal on semiconductor nanoparticles is an essential factor for maximizing the efficiency of photocatalytic reactions. A noble metal (e.g., Pd), which acts as a sink for photoinduced charge carriers, promotes interfacial charge-transfer processes.

The TiO_2 lattice with metal ions such as iridium cations intro- duces new energy levels in the band gap which can be tailored to extend photosensitivity in the visible light region. By doping of metal or nonmetal ions, the properties of the functional materials are modified. For example, S- or N-doped TiO_2 has shown a relatively high photoactivity under visible light irradiation [21–23]. However, Ir-doped brookite TiO_2 showed the highest photonic efficiency among the materials tested under visible light irradiation.

The importance of modifying the shape of a TiO_2 structure by controlling the morphology of TiO_2 particles was confirmed in pre- vious works [24], which promotes an effective electron–hole pair charge separation. In this work, we synthesized Ir-doped brookite TiO_2 nanoparticles with high crystallinity by using a microwave synthesis process. The surface area of the prepared TiO_2 was increased by increasing the amount of Ir cations as a dopant. A higher photocatalytic activity than that of the tested commercial doped photocatalysts was exhibited presumably due to the high crystallinity and high surface area. With a high specific surface area, the possibility of O_2 reduction producing $O_2^{\bullet-}$ radicals is higher [25]. In addition to this, brookite TiO_2 has been reported to show good performance under UV light for decomposition of acetaldehyde [26]. In the present study, Ir-doped brookite TiO_2 as a photocatalyst could decompose acetaldehyde or toluene under pure visible light irradiation (入 455 nm).

4.2. Dopant and light absorption band

UV–vis spectra were used to clarify the light absorption edge of the TiO_2 brookite material as well as band gap calculation through the reflectance function for an indirect semiconductor. The band gaps of the prepared samples were 3.14 eV and 1.88 eV before and after 0.5 wt% Ir-doping, respectively. Experimental band gap ener- gies of brookite TiO_2 have been reported to range from 3.14 eV [6,27,28] to 3.4 eV [8]. The obtained band gap of the pure brookite TiO_2 in this study is consistent with results of previous studies [6,27,28]. Ir cations were shown to be incorporated in the lattice of brookite TiO_2 by XPS analyses after Ar etching treatment. Sev- eral runs were conducted with the same Ir-doped TiO_2 brookite material without any detriment in its photocatalytic performance.

4.3. Proposed mechanism

In relation to our characterized self-synthesized Ir-doped TiO_2 photocatalyst and according to oxidation potential values of toluene (1.276 V vs NHE) [29] and acetaldehyde (0.6 V vs NHE) [30], a photocatalytic reaction mechanism under visible light irradiation was proposed. The linked pathways are confirmed from the obtained CO_2 evolution. When Ir-doped TiO_2 was irradiated under visible light, h^+ from the photogenerated pairs e^-/h^+ in the doped particles is quickly trapped in the deep trapping sites, that is, the doping sites [23]. Meanwhile, the photogenerated conduction

band electrons will migrate to the surface to the reduction site of the par- ticle, where the main process of photo-reduction of O_2 takes place to produce superoxide $O_2^{\bullet-}$ radicals (Fig. 10).

The flat band potential of the brookite TiO_2 was estimated by a Mott-Schottky plot to be −0.766 V (vs Ag/AgCl). Therefore, the calculated conduction band (CB) should be −0.51 V (vs NHS) at pH 7, the potential of which is sufficient to reduce O_2 adsorbed on the surface of Ir-doped brookite TiO_2, resulting in production of superoxide radicals under visible light irradiation. The produced superoxide radicals are thought to be responsible for the pro- duction of surface-adsorbed H_2O_2 molecules [31], which might produce the formally trapped $^\bullet OH$ radical, Ti-$^\bullet OH$. Therefore, super-oxide radicals play an important role in decomposition of organic compounds. It has been reported that N-doped TiO_2 [32,33] and S-doped TiO_2 [34] cannot generate free $^\bullet OH$ radicals under visible light irradiation and therefore have limited oxidative power.

It is plausible that free $^\bullet OH$ radicals diffuse through an oxida-tive path to the gas phase from the photocatalytic TiO_2 surface under UV light irradiation [31]. In our case, it might not be possible to produce free $^\bullet OH$ radicals by the midgap state due to the lack of oxidation potential under visible light. Highly reactive free $^\bullet OH$ radicals require strong redox potential conditions to be produced and released. A compound suitable for producing free $^\bullet OH$ radicals through the oxidative valence band holes is, for example, modified WO_3 with TiO_2 or Pt as co-catalysts under visible light, because its band gap lies on an appropriate redox potential position [35,36].
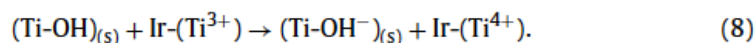
A certain amount of Ir^{III} cations in the lattice of TiO_2 was reduced to generate Ir^{II} cations by photogenerated electrons. After irradia- tion, the color of the Ir-doped TiO_2 photocatalyst changed from yellow to an almost brown color. The difference in the color is probably due to the change in oxidation level of iridium [37]. This phenomenon was confirmed by XPS and UV spectra before and after irradiation.

The initial steps in the photocatalytic process prior the initiation of acetaldehyde or toluene degradation are as follows [Equations (6)–(10)].

Charge separation:

$$Ir\text{-}(TiO_2) \xrightarrow{vis\text{-}h\nu} e^- + h^+. \tag{6}$$

Charge transfer of positive charge:

$$h^+ + OH^-_{(s)} \rightarrow (Ti - OH)_{(s)}, \tag{7}$$

$$(Ti\text{-}OH)_{(s)} + Ir\text{-}(Ti^{3+}) \rightarrow (Ti\text{-}OH^-)_{(s)} + Ir\text{-}(Ti^{4+}). \tag{8}$$

Electron transfer reactions:

$$e^- + O_2 \rightarrow O_2^-, \tag{9}$$

$$O_2^{\bullet-} + H^+ \rightarrow HO_2^\bullet \tag{10}$$

The superoxide radicals and Ti-$^\bullet OH$ should be important reac- tants that interact and promote decomposition of pollutants on the surface. It has been reported that TiO_2 particles after H_2O_2 treatment increase the absorption range up to visible light due to generation of surface peroxide species [38]. For this reason, Equation (7) represents particular importance to the proposed mechanism. From the oxidation potential and reaction potential, Ti-·OH is thought to be predominant active species for degradation of organic compounds. In a previous work was shown the importance of oxidation sites on the surface [39].

2. Conclusions

Visible light-active Ir-doped brookite TiO_2 photocatalysts were successfully synthesized by using different concentrations of irid- ium metal in a hydrothermal assisted-microwave system. The synthesis procedure by application of a microwave can be consid- ered a green process with low energy and fast synthesis reactions within 7 min to obtain brookite TiO_2 instead of the 48 h required by the traditional hydrothermal method. The reaction period in the microwave is relevant since the brookite structure will

be well formed by 7 min. A shorter time of reaction does not form a crys- talline brookite. The reaction time can be increased over 7 min and the brookite sharpness increases but no significant change was observed.

A wide range of visible light absorption was confirmed by reflectance spectra analyses and by band-gap calculations. TEM images as well as XRD patterns showed a high level of crys- tallinity of the doped photocatalysts. These results indicate that crystallinity of the prepared TiO_2 is one of the important factors for exhibiting high photocatalytic activity.According to the BET study, the doped photocatalysts showed a much larger surface area than that of the undoped brookite TiO_2. For photocatalytic decom- position of acetaldehyde or toluene in gas phase, Ir-doped TiO_2

brookite showed remarkable photocatalytic activities under visible light irradiation (入 455 nm). The

highest photonic efficiency of Ir-

doped brookite TiO_2 over commercial available photocatalysts was observed under visible light when 0.5 wt% Ir cations were doped into the lattice of brookite TiO_2.

Acknowledgements

References

[1] C.G. Granqvist, Sol. Energy Mater. Sol. Cells 91 (2007) 1529–1598.

[2] K. Tomita, V. Petrykin, M. Kobayashi, M. Shiro, M. Yoshimura, M. Kakihana, Angew. Chem. 118 (2006) 2438–2441.

[3] E.P. Meagher, G.A. Lager, Can. Mineral 17 (1979) 77–85.

[4] L. Pauling, J.H. Sturdivant, Z. Kristallogr. 68 (1928) 239–256.

[5] H. Kominami, M. Kohno, Y. Kera, J. Mater. Chem. 10 (2000) 1151–1156.

[6] H. Kominami, Y. Ishii, M. Kohno, S. Konishi, Y. Kera, B. Ohtani, Catal. Lett. 91 (2003) 41–47.

[7] R. Buonsanti, V. Grillo, E. Carlino, C. Giannini, T. Kipp, R. Cingolani, P.D. Cozzli, J. Am. Chem. Soc. 130 (2008) 11223–11233.

[8] W. Hu, L. Li, G. Li, C. Tang, L. Sun, Cryst. Growth Des. 9 (2009) 3676–3682.

[9] T.A. Kandiel, A. Fledhoff, L. Robben, R. Dillert, D.W. Bahnemann, Chem. Mater. 22 (2010) 2050–2060.

[10] A. Di Paola, M. Bellardita, L. Palmisano, Catalysts 3 (2013) 36–73.

[11] L. Atanasoska, P. Gupta, C. Deng, R. Warner, S. Larsen, J. Thomson, ECS Trans. 16 (2009) 37–48.

[12] M. Tsuji, M. Hashimoto, Y. Nishizawa, M. Kubokawa, T. Tsuji, Chem. Eur. J. 11 (2005) 440– 452.

[13] P. Zhang, S. Yin, T. Sato, Appl. Catal. B 89 (2009) 118–122.

[14] Y. Morishima, M. Kobayashi, V. Petrykin, M. Kakihana, K. Tomita, J. Ceram. Soc. Jpn. 115 (2007) 826–830.

[15] S. Horikoshi, M. Abe, S. Sato, N. Serpone, J. Photochem. Photobiol. A 220 (2011) 94–101.

[16] C. Baumannis, D.W. Bahnemann, J. Phys. Chem. C 112 (2008) 19097–19101.

[17] V.M. Menéndez-Flores, Developing Nanoparticles for Decomposition of Toxic Compounds, Südwestdeutscher Verlag für Hochschulschriften, AG Co. KG, ISBN 978-3-8381-1953-3, 2010, p. 188.

[18] N. Serpone, A. Salinaro, Pure Appl. Chem. 71 (1999) 303–320.

[19] V.M. Menéndez-Flores, D. Friedmann, D.W. Bahnemann, Int. J. Photoenergy 2008 (2008) 11.

[20] G. Liu, L. Wang, H. Gui Yang, H.M. Cheng, G. Qing Lu, J. Mater. Chem. 20 (2009) 831–843.

[21] T. Ohno, Z. Miyamoto, K. Nishijima, H. Kanemitsu, F. Xueyuan, Appl. Catal. A 302 (2006) 62– 68.

[22] K. Nishijima, T. Kamai, N. Murakami, T. Tsubota, T. Ohno, Int. J. Photoenergy 2008 (2008) 7.

[23] V.M. Menéndez-Flores, D.W. Bahnemann, Teruhisa Ohno, Appl. Catal. B 103 (2011) 99–108.

[24] V.M. Menéndez-Flores, M. Nakamura, T. Kida, Z. Jin, N. Murakami, T. Ohno, Appl. Catal. A 406 (2011) 119–123.

[25] T. Daimon, T. Hirakawa, M. Kitazawa, J. Suetake, Y. Nosaka, Appl. Catal. A 340 (2008) 169–175.

[26] N. Murakami, T. Kamai, T. Tsubota, T. Ohno, Catal. Commun. 10 (2009) 963–966.

[27] D. Reyes-Coronado, G. Rodríguez-Gattorno, M.E. Espinosa-Pesqueira, C. Cab, R. de Coss, G. Oskam, Nanotechnology 19 (2008) 145605–145614.

[28] M. Grätzel, F. Rotzinger, Chem. Phys. Lett. 118 (1985) 474–477.

[29] E. Li, G. Shi, X. Hong, P. Wu, J. Appl. Polym. Sci. (2004) 189–195.

[30] T. Arai, M. Yanagida, Y. Konishi, Y. Iwasaki, H. Sugihara, K. Sayama, J. Phys. Chem. Lett. 111 (2007) 7574–7577.

[31] Y. Murakami, K. Endo, I. Ohta, A.Y. Nosaka, Y. Nosaka, J. Phys. Chem. C 111 (2007) 11339–11346.

[32] M. Mrowetz, W. Balcerski, A.J. Colussi, M.R. Hoffmann, J. Phys. Chem. B 108 (2004) 17269–17273.

[33] T. Hirakawa, Y. Nosaka, J. Phys. Chem. C 112 (2008) 15818–15823.

[34] T. Tachikawa, S. Tojo, K. Kawai, M. Endo, M. Fujitsuka, T. Ohno, K. Nishijima, Z. Miyamoto, T. Majima, J. Phys. Chem. B 108 (2004) 19299–19306.

[35] J. Kim, C. Wee Lee, W. Choi, Environ. Sci. Technol. 44 (2010) 6849–6854.

[36] V. Iliev, D. Tomova, S. Rakovsky, A. Eliyas, G. Li Puma, J. Mol. Catal. A: Chem. 327 (2010) 51–57.

[37] J. Yano, K. Noguchi, S. Yamasaki, S. Yamazaki, Electrochem. Commun. 6 (2004) 110–114.

[38] T. Ohno, Y. Masaki, S. Hirayama, M. Matsumura, J. Catal. 204 (2001) 163–168.

[33] L. Zhang, V.M. Menéndez-Flores, N. Murakami, T. Ohno, Appl. Surf. Sci. 258 (2012) 5803–5809.